

Ratio of kaon-to-pion production cross-sections in *BeBe* collisions as a function of \sqrt{s}

G.I. Lykasov, A.I. Malakhov, A.A. Zaitsev

Joint Institute for Nuclear Research, Dubna 141980, Moscow region, Russia

lykasov@jinr.ru
malakhov@lhe.jinr.ru
zaicev@jinr.ru

Abstract

The inclusive spectra of pions and kaons produced in *BeBe* collisions as functions of their transverse momentum p_t at mid-rapidity are calculated within the self-similarity approach. A satisfactory description of NA61/SHINE data on these spectra and the ratio of K^\pm to π^\pm meson production cross sections in *BeBe* collisions as a function of \sqrt{s} are presented. The similarity of these observables to the ones for *pp* collisions at mid-rapidity and in the wide range of initial energies is illustrated

1 Introduction

The investigation of strange hadron and pion production in heavy-ion collisions is a promising tool to search for new physical properties of such processes. The

observation of a sharp peak in the production ratio of K^+ mesons to π^+ mesons in central $Pb + Pb$ and $Au + Au$ collisions at mid-rapidity [1, 2] has attracted the attention of both theoreticians and experimentalists see [3]- [20] and references therein. When the initial energy $\sqrt{s_{NN}}$ per nucleon becomes larger than 30 GeV this ratio falls down. However, the ratio of K^+ to π^+ mesons produced in collisions of nuclei lighter than Pb and Au , as a function of the initial energy $\sqrt{s_{NN}}$ per nucleon, in particular, $Be + Be$ [17] and $Ar + Sc$ [18] has no peak. The fast increase of this ratio, when $\sqrt{s_{NN}}$ grows from the kaon threshold up to 20-30 GeV and the slow increase at larger energies has been observed [17, 19]. A similar energy dependence is observed by the NA61/SHINE Collaboration in $BeBe$ and $ArSc$ collisions. Moreover, the energy dependence of K/π ratios observed in $BeBe$ collisions [17] is similar to the one in pp collisions.

In this paper we analyze the production of kaons and pions in $BeBe$ collisions at mid-rapidity and focus on ratios between their cross-sections as functions of the initial energy within the same theoretical approach, which was presented in [21] for pp collisions. This approach is based on the similarity of spectra of hadrons produced in AA collisions at zero rapidity $y = 0$ and on the conservation laws of four-momenta and quantum numbers suggested in [22–25]. It was a continue of the approach suggested earlier in pioneering papers [27–30]. Further development of this approach was presented in [21, 26, 31–33].

2 Main properties of the self-similarity approach for AA collisions.

The inclusive production of hadron 1 in the interaction of nucleus A with nucleus B

$$A + B \rightarrow 1 + \dots, \quad (1)$$

is satisfied by the conservation law of four-momenta in the following form [24, 25]:

$$(N_A P_A + N_B P_B - p_1)^2 = (N_A m_0 + N_B m_0 + M)^2, \quad (2)$$

where N_A and N_B are the fractions of the four-momentum transmitted by nucleus A and nucleus B , the forms of N_A, N_B are presented in [25, 32]; P_A, P_B, p_1 are the four-momenta of nuclei A and B and particle 1, respectively; m_0 is the mass of the free nucleon; M is the mass of the particle providing for conservation of the baryon number, strangeness, and other quantum numbers. Eq. 2 was introduced

in [24,25] for the production of hadrons in AB collisions in the kinematics forbidden for free nucleon-nucleon collisions. In fact, it is valid for initial energies of colliding nuclei close to the threshold of hadron production. It allows us to find the minimal value of M , which provides for the conservation of quantum numbers. For π -mesons $m_1 = m_\pi$ and $M = 0$. For anti nuclei $M = m_1$ and for K^- -mesons $M = m_1 = m_K$, m_K is the mass of the K -meson. For nuclear fragments $M = -m_1$. For K^+ -mesons $m_1 = m_K$ and $M = m_\Lambda - m_0$, m_Λ is the mass of the Λ -baryon. Let us note that the isospin effects of the produced hadrons and other nuclear effects are out of this approach. Therefore, it is assumed that within the self-similarity approach there is no big difference between the inclusive spectra of π^+ and π^- mesons produced in pp and AA collisions. However, there is a difference between similar spectra of K^+ and K^- mesons, because the values of M are different. This is due to the conservation law of strangeness.

In [24,25] the parameter of self-similarity is introduced in the following form:

$$\Pi = \min \frac{1}{2} \left[(u_A N_A + u_B N_B)^2 \right]^{1/2}, \quad (3)$$

where u_A and u_B are the four-velocities of nuclei A and B . The minimization over N presented in Eq. (3) allows us to find the parameter Π . This parameter introduced in [24] was obtained in [25] for nucleus-nucleus collisions in the mid-rapidity region, however, it can also be applied successfully for the analysis of pion production in pp collisions, as it was shown in [31–33].

The inclusive spectrum of particle 1 produced in the AB collision can be parameterized as a general universal function dependent on the self-similarity parameter Π , as it was shown in [26].

$$Ed^3\sigma_{AB}/d^3p = A_A^{\alpha(N_A)} \cdot A_B^{\alpha(N_B)} \cdot F(\Pi) \quad (4)$$

where $\alpha(N_A) = 1/3 + N_A/3$, $\alpha(N_B) = 1/3 + N_B/3$ and function $F(\Pi)$ is the inclusive spectrum of hadron production in the NN collision [32, 33], A_A and A_B is the number of nucleons in nuclei A and B , respectively.

The form of Eq. 4 allowed us to describe satisfactorily inclusive spectra of hadrons produced in pA and AB collisions in kinematics forbidden at hadron production in pp interactions and of particles produced close to the threshold of nucleon-nucleon collisions. This form of the inclusive hadron spectrum also results in the satisfactory description of p_t spectra of pions produced in AB collisions at the mid-rapidity region and not large transverse momenta p_t of produced pions in the wide range of initial energies [31–33, 38]. Therefore, we apply it to

describe p_t spectra of kaons produced in AB collisions at mid-rapidity and not large transverse momenta.

For symmetric colliding nuclei $N_A = N_B = N$ the function Π is found from the minimization of Eq. 3 by solving the equation. This assumption has been suggested in [24, 25]

$$\frac{d\Pi}{dN} = 0 \quad (5)$$

The exact solution of Eq. 5 at zero rapidity $y = 0$, as $N = \Pi / \cosh(Y) \equiv 2m_0\Pi / \sqrt{s}$, was obtained in [25], for details see, also [32]. Therefore, $\alpha(N) = 1/3 + 2m_0\Pi / (3\sqrt{s})$. For symmetric nuclei Eq. 4 is presented in the following form

$$Ed^3\sigma_{AA}/d^3p = A^{2\alpha(N)} \cdot F(\Pi) \quad (6)$$

$$F(\Pi) = \left[A_q \exp\left(-\frac{\Pi}{C_q}\right) + A_g \sqrt{p_T} \phi_1(s) \exp\left(-\frac{\Pi}{C_g}\right) \right] \sigma_{tot} \quad (7)$$

where

$$\Pi(s, m_{1T}, y) = \left\{ \frac{m_{1T}}{2m_0\delta_h} + \frac{M}{\sqrt{s}\delta_h} \right\} \cosh(y)G, \quad (8)$$

$$G = \left\{ 1 + \sqrt{1 + \frac{M^2 - m_1^2}{(m_{1T} + 2Mm_0/\sqrt{s})^2 \cosh^2(y)} \delta_h} \right\}.$$

Here $\phi_1(s) = 1 - \sigma_{nd}(s)/\sigma_{tot}(s)$, see [32, 33],

$\delta_h = \left(1 - \frac{s_h}{s}\right)$; $s_{th}^\pi \simeq 4m_0^2$; $s_{th}^{K^+} = (m_0 + m_K + m_\Lambda)^2$; $s_{th}^{K^-} = (2m_0 + 2m_K)^2$; $M = m_\Lambda - m_0$; $m_\Lambda = 1.115$ GeV; $m_K = 0.494$ GeV; $s_0 = 1$ GeV; $m_0 = 0.938$ GeV; p_{1T} and m_{1T} are the transverse momentum and transverse mass of the produced hadron 1; $\sigma_{nd} = (\sigma_{tot} - \sigma_{el} - \sigma_{SD})$ is the non-diffractive cross-section; σ_{tot} , σ_{SD} and σ_{el} are the total cross-section, the single diffractive cross section and the elastic cross-section of pp collisions, respectively. They were taken from [39] and [40] and, together with parameters A_q, C_q and A_g, C_g , they are presented in the Appendix.

Note, the self-similarity parameter Π depends not only on the transverse mass m_{1T} and the rapidity y of the produced hadron but also on the initial energy \sqrt{s} . It leads to the non factorized form of the inclusive spectrum presented as Eqs. (4,6),

as a function of s, m_T, y . At large \sqrt{s} the energy dependence of Π vanishes. This is the main difference of this approach from another models.

In fact, the function $F(\Pi)$ in Eq. (7) is the inclusive spectrum of hadrons produced in pp collisions at the mid-rapidity ($y \simeq 0$), which was calculated within the approach suggested in [35, 36]. The form of $F(\Pi)$ is due to the quark contribution (the first term of Eq. (7)) and the contribution of nonperturbative gluons (the second term of Eq. (7)). The forms of $F(\Pi)$ and $Ed^3\sigma_{AA}/d^3p$ allowed us to describe satisfactorily the data on inclusive spectra of hadrons produced in pp and AA collisions at $y \simeq 0$ and the wide range of the initial energies \sqrt{s} [21, 31–33]. From the best description of the inclusive spectrum of charged hadrons produced in pp collisions at LHC energies the transverse momentum dependence on the gluon density (TMD) at low square transfers Q^2 was constructed in [36]. The use of it allowed us to describe rather satisfactorily LHC data on hard pp processes, HERA data on deep inelastic scattering (DIS) and ZEUS data on the charmed and bottom structure functions F_{2c}, F_{2b} [37, 38]. Therefore, we can quite reasonably apply $F(\Pi)$ in the form of Eq. (7) entered into Eq. 6 to analyze the p_t spectra of hadrons produced in AA collisions at the mid-rapidity range at not large p_t .

3 Results and discussion

In the case of the process $AA \rightarrow h + X$ Eq. 4 looks as the following:

$$\begin{aligned} \rho_{AA}^h(p_{hT}, y) &\equiv E_h \frac{d^3\sigma_{AA}^h}{d^3p_1} = \frac{1}{\pi} \frac{d\sigma_{AA}^h}{dp_{1T}^2 dy} = \\ &\frac{1}{\pi} \frac{d\sigma_{AA}^h}{dm_{1T}^2 dy} = A^{2\alpha(N)} F(\Pi(s, m_{1T}, y)), \end{aligned} \quad (9)$$

Then, the production cross-section of hadron h in AA collisions integrated over its transverse momentum p_{1T} or transverse mass m_{1T} at zero rapidity $y = 0$ and $s \geq s_{th}^h$ can be presented in the following form:

$$\frac{d\sigma_{AA}^h}{dy}(s, y = 0) = 2\pi \int_{p_{1T}^{\min}}^{p_{1T}^{\max}} \rho_{h_1}^{AA}(s, p_{1T}, y = 0) p_{1T} dp_{1T} \quad (10)$$

Then, the ratio of production cross-sections for hadrons h_1 and hadrons h_2 in AA collisions and at $y = 0$ as \sqrt{s} can be presented in the following form:

$$R_{AA}^{h_1 h_2} = \frac{d\sigma_{AA}^{h_1}}{dy}(s, y = 0) / \frac{d\sigma_{AA}^{h_2}}{dy}(s, y = 0) \quad (11)$$

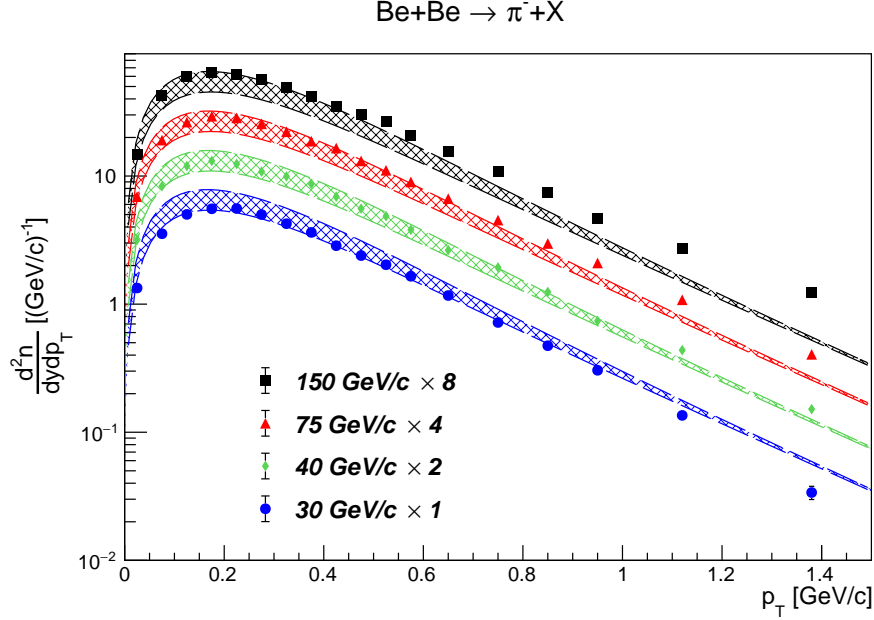


Figure 1: The p_T -spectra of π^- mesons produced in the 20% most central $BeBe$ collisions at momenta of the initial Be nucleus $P_{in} = 150A$ GeV/c ($\sqrt{s}=16.84$ GeV per nucleon), $75A$ GeV/c ($\sqrt{s} = 11.94$ GeV per nucleon), $40A$ GeV/c ($\sqrt{s} = 8.77$ GeV per nucleon), $30A$ GeV/c ($\sqrt{s} = 7.68$ GeV per nucleon) at mid-rapidity $y < 0.2$. The lines are our calculations, the data are taken from [54] and normalized to 20% of centrality. The bands are due to uncertainties in parameter A_q presented in the Appendix.

The p_T -spectra of π^- , K^+ and K^- mesons are the sums of quark and gluon contributions including uncertainties due to the fit of data that are presented in Figs. (1-3). By fitting NA61/SHINE data on p_T -spectra at mid-rapidity the parameters C_q , A_q , C_g were found to be independent of the initial energy \sqrt{s} , they depend on the kind of mesons produced, π , K^+ , K^- . However, the parameter A_q varies a little bit at energies between $40A$ GeV/c and $150A$ GeV/c. The uncertainties in p_T -spectra and ratios of yields, K^+/π^+ and K^-/π^- , are due to the uncertainties in the parameter A_q . All these parameters are presented in the Appendix. Similar spectra with quark and gluon contributions are also presented in the Appendix.

In Figs. (4,5) the respective yield ratios, K^+/π^+ and K^-/π^- , are presented as functions of \sqrt{s} . From these figures one can see their fast rise from the threshold

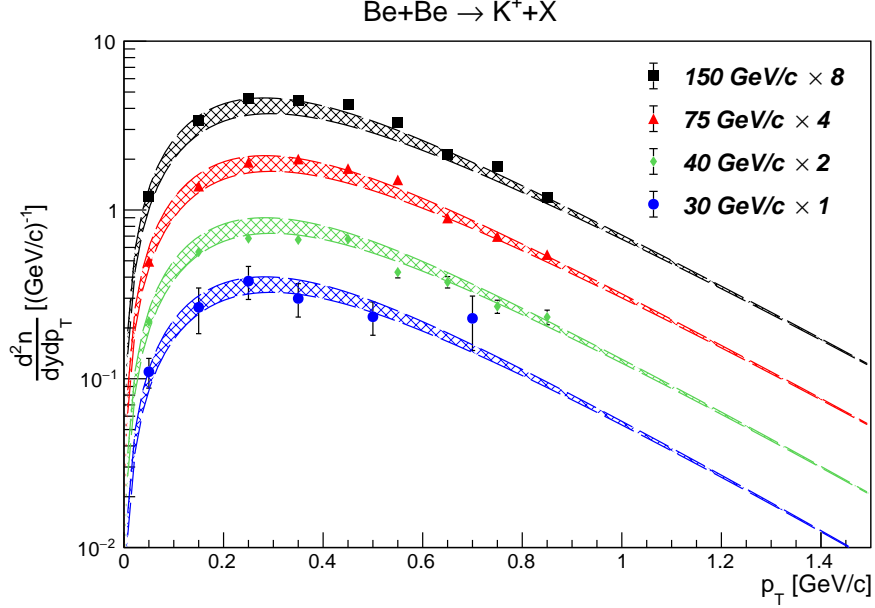


Figure 2: The p_T -spectra of K^+ mesons produced in central $BeBe$ collisions. Notations are the same as in Fig. 1. The NA61/SHINE data were taken from [17].

energy of K^+ or K^- production up to $\sqrt{s} = 20\text{-}30$ GeV and their further slow increase with energy.

The upper line in Fig. 4 corresponds to the fit of data for π^+ and K^+ mesons at $P_{in} = 30A$ GeV/c, and the lower line corresponds to the similar fit at $P_{in} = 75A$ GeV/c. The upper curve in Fig. 5 corresponds to the fit of data for π^- and K^- mesons at $P_{in} = 30A$ GeV/c and the lower line corresponds to the similar fit at $P_{in} = 75A$ GeV/c.

The p_T -spectra of pions and kaons produced in the mid-rapidity of $BeBe$ collisions and their ratios K/π as functions of \sqrt{s} were calculated within different models: Epos 1.99 [6,7], URQMD 3.4 [8,9], AMPT 1.26 [10–12], PHSD 4.00 [13,14], SMASH 1.6 [15,16]. In [17] the comparison of results obtained within these models at the center rapidity region $y = 0$ with the NA61/SHINE data was performed. It was illustrated in Figs.(34,35) of this paper that all these models do not result in the total description of the NA61/SHINE data at the initial momentum about 150A GeV/c. The energy dependence of the cross sections ratio K/π at $y = 0$ is described more less satisfactorily within the URQMD model [8,9], see Fig.37

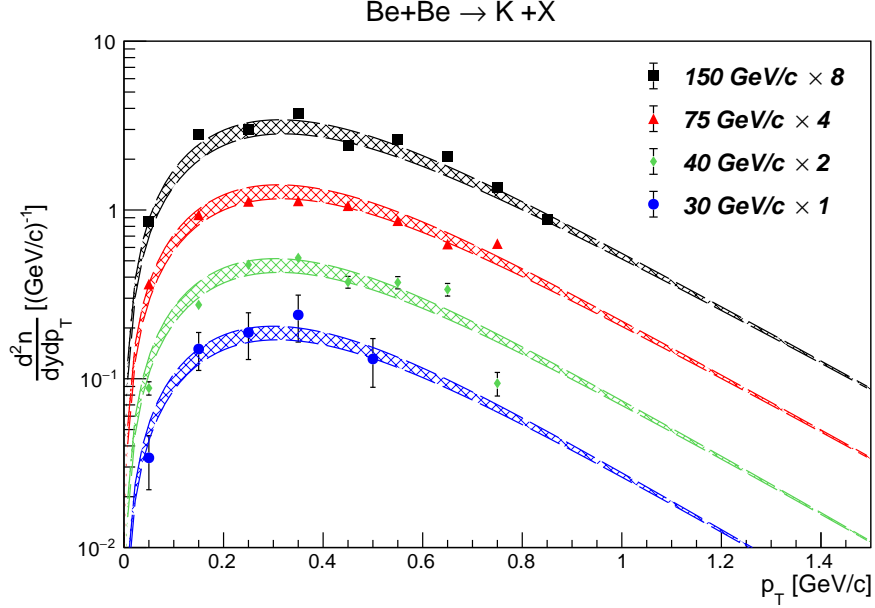


Figure 3: The p_T -spectra of K^- mesons produced in central $BeBe$ collisions. Notations are the same as in Fig. 1. The NA61/SHINE data were taken from [17].

of [17]. However, this URQMD model does not describe the p_T and y spectra of pions and kaons satisfactorily at the initial momentum about 150A GeV/c, as it is seen from Figs.(34,35) of the NA61/SHINE paper.

4 Conclusion

In this paper we have applied the self-similarity approach to analyze the production of both kaons and pions in $BeBe$ collisions at mid-rapidity $y < 0.2$ within a wide range of initial energies. We have presented a self-consistent satisfactory description of the NA61/SHINE data on p_T -spectra of pions and kaons at $7.62 \leq \sqrt{s} \leq 16.84$ GeV. The fast rise of the K^+/π^+ and K^-/π^- yield ratios as functions of \sqrt{s} from the threshold energy of K^+ or K^- production up to $\sqrt{s} = 20$ -30 GeV has been demonstrated as well as their further slow increase with growing energy. The ratio of kaon yields to those of pions, produced in $BeBe$ collisions, has been calculated within this approach as a function of \sqrt{s} .

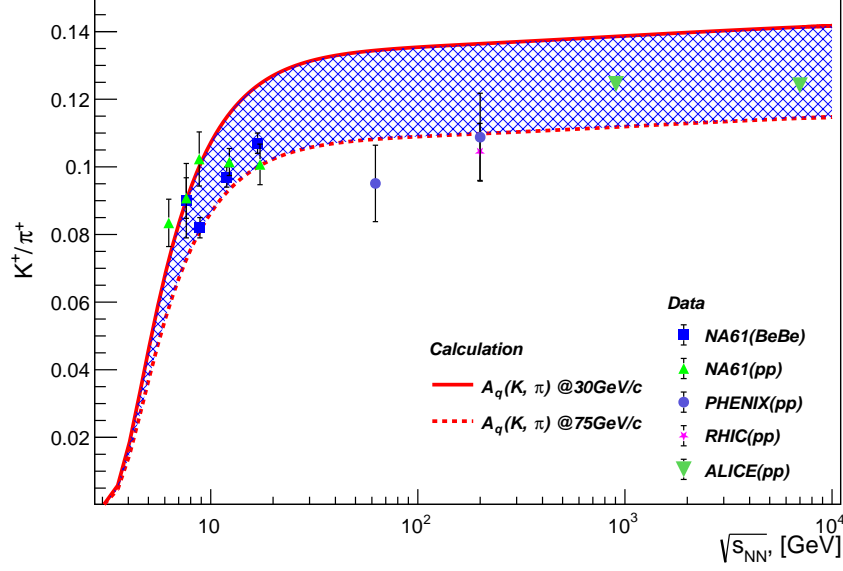


Figure 4: The ratio of K^+ and π^+ meson yields produced in the mean-rapidity of $BeBe$ (NA61/SHINE) [17] and pp (NA61/SHINE, PHENIX, STAR, ALICE) [49–53] collisions as a function of \sqrt{s} .

The energy dependence of the ratio of kaon yields to those of pions in $BeBe$ collision is the same as in pp collision considered earlier in [21]. The fast rise with energy of the kaon and pion production cross-sections, when \sqrt{s} grows from the threshold energy, is due to the conservation law of the four-momenta of initial and produced particles and the factor $\delta_h = 1 - s_{th}^h/s$ entering into the self-similarity function $\Pi(s, m_{1T}, y)$ given by Eq.(7). The non-zero value of M in the kaon production cross-section results in the fast rise of the K^\pm/π^\pm yield ratios because in the pion production cross-section $M = 0$. When $\sqrt{s} \gg \sqrt{s_{th}}$ and $\sqrt{s} \gg M$, the pion and kaon production cross-sections and their ratios become insensitive to factors δ_h and M , however, they are sensitive to the difference between the quark and gluon contributions to the pion and kaon spectra as functions of p_T and \sqrt{s} . That is why the K^\pm/π^\pm yield ratios exhibit two kinds of energy dependence, a fast rise, when $\sqrt{s_{th}} < \sqrt{s} < 20\text{--}30$ GeV and a slow increase, when $\sqrt{s} > 20\text{--}30$ GeV.

Let us note that no fast rise and no sharp peak in the ratio between the yields of K^+ and π^+ mesons produced in central $BeBe$ collisions are observed in the

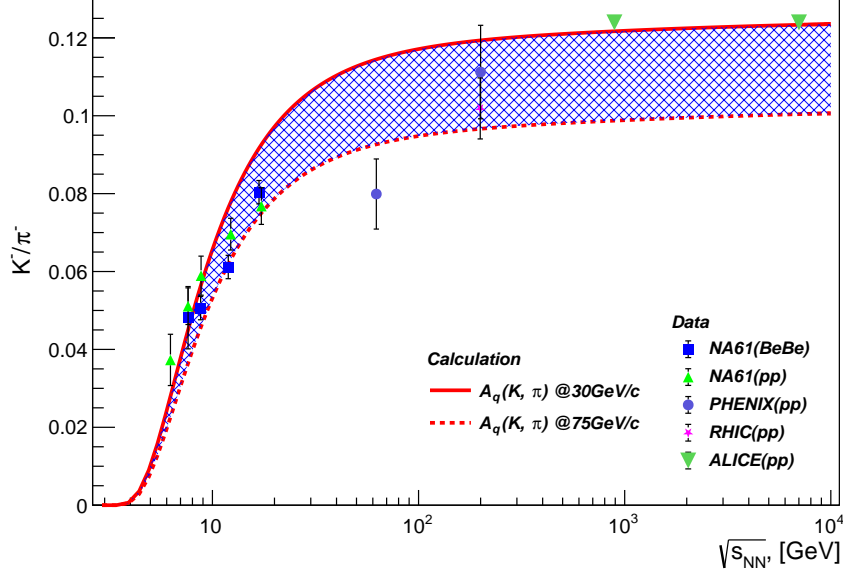


Figure 5: The ratio of K^- and π^- meson yields produced in $BeBe$ (NA61/SHINE) [17] and pp (NA61/SHINE, PHENIX, STAR, ALICE) [49–53] collisions as a function of \sqrt{s} .

NA61/SHINE experiment, according to [17]. This ratio is very similar to the same K^+/π^+ ratio measured in pp collisions by the NA61/SHINE Collaboration.

5 Appendix

The parameterizations of σ_{tot} , σ_{SD} and σ_{el} have the following forms [39] and [40]
 $\sigma_{tot} = (21.7(s/s_0)^{0.0808} + 56.08(s/s_0)^{-0.4525})$ mb;
 $\sigma_{el} = (12.7 - 1.75\ln(s/s_0) + 0.14\ln^2(s/s_0))$ mb;
 $\sigma_{SD} = (4.2 + \ln(\sqrt{s/s_0}))$ mb.

In Fig. 6 the p_T -spectra of pions and kaons, produced in the mid-rapidity of $BeBe$ collisions within the initial momentum range of (30-150) GeV/c, fitted by the NA61/SHINE data, are presented. The black dashed line corresponds to the quark contribution, the blue dash-dotted curve is the gluon contribution and the red solid line is the sum of quark and nonperturbative gluon contributions. The

parameters A_q, A_g and C_q, C_g were found from a fit of NA61/SHINE data and are presented in Table 1.

As it is shown in [31–33], the form of inclusive pion spectra versus p_T at mid-rapidity given by Eqs. (6-8) describes satisfactorily data in a wide range of \sqrt{s} at $p_T < 2-3$ GeV/c. Moreover, as it is shown in [35–37] and [38], the contribution of gluons to the pion spectrum is related to the gluon distribution at low $Q^2 = 1-2$ (GeV/c)², the use of which results in a satisfactory description of data on hard pp processes at LHC energies and of proton structure functions at low x . Therefore, we use Eqs. (4-7) for the description of data on pion p_T -spectra in $BeBe$ collisions, only improving the fit of data.

As for K^\pm production in $BeBe$ collisions at not large initial energies we take into account the additional contribution due to the one Reggeon exchange diagram, which has a $\sqrt{s_{th}/s}$ dependence. It leads to modification of parameter A_q in the following form $A_q(1 + \sqrt{s_{th}/s})$, which can be approximated by $A_q \exp(\sqrt{s_{th}/s})$. This correction vanishes at RHIC and LHC energies, however, it allows us to describe data at $\sqrt{s} < 10$ GeV satisfactorily.

Parameters A_q for π, K^+ and K^- meson production were found from the fit of NA61 data [17, 54] at initial energies $P_{in} = 30A-150A$ GeV/c. Parameters A_g for π, K^+ and K^- meson production were found from the fit of NA61 data at $P_{in} = 150A$ GeV/c. Other parameters C_q and C_g were taken from fits of NA61 data in pp collisions.

Table 1: Table of parameters found from the fit of NA61/SHINE data.

Be+Be→ $h + X$	π^-				K^+				K^-			
$\sqrt{s_{pp}}, \text{ GeV}$	16.8	11.9	8.8	7.6	16.8	11.9	8.8	7.6	16.8	11.9	8.8	7.6
$P, \text{ GeV/c}$	150	75	40	30	150	75	40	30	150	75	40	30
A_q	17.7	15.9	13.9	11.7	3.8	3.3	2.7	3.2	9.1	7.9	7.1	7.5
C_q	0.147				0.148							
A_g	6.85				2.963							
C_g	0.22				0.2271							

Acknowledgements.

We are very grateful to K.A. Bugaev, M. Gumberidze, M. Gazdzicki, R. Holzmann, S. Pulawski, G. Pontecorvo for extremely helpful discussions.

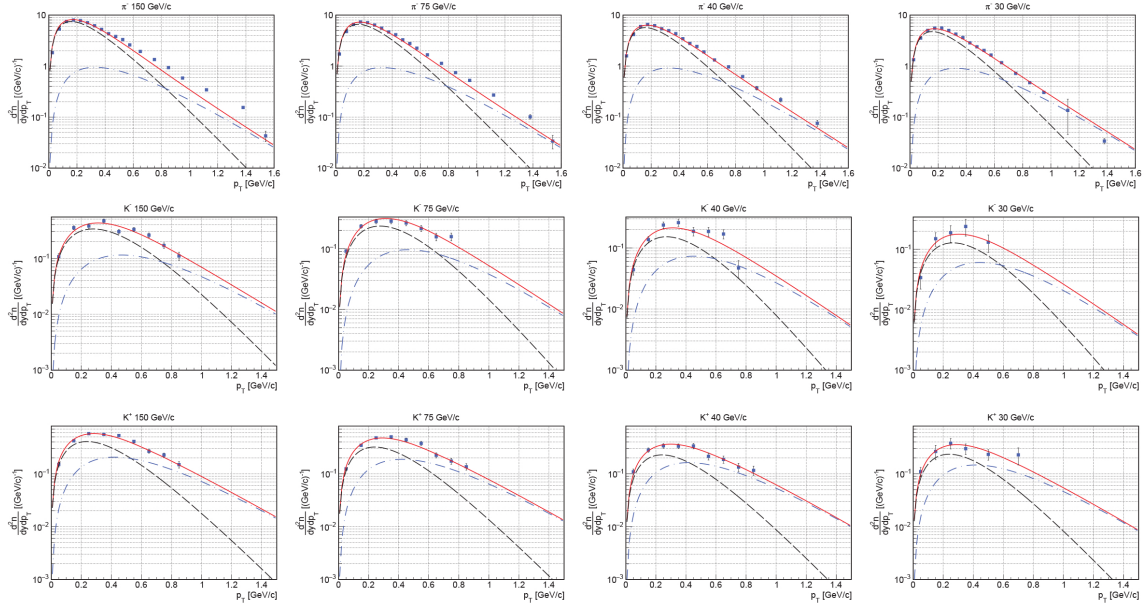


Figure 6: The p_T spectra of π^- , K^+ and K^- mesons produced at $y \approx 0$ in inelastic $BeBe$ interactions at SPS energies $\sqrt{s} = 7.68 - 16.84$ GeV or $P_{in} = 30-150$ GeV/c. The NA61/SHINE data were taken from [17, 54].

References

- [1] S.V. Afanasiev, et al., (NA49 Collaboration) Phys.Rev.C **66**, 054902 (2002).
- [2] C. Alt, et al., (NA49 Collaboration) Phys.Rev.C **77**, 024903 (2008).
- [3] M. Gazdzicki, M.I. Gorenstein, Acta Physica Polon., B **30**, 2705 (1999).
- [4] M. Gazdzicki, M.I. Gorenstein, P. Seyboth, J.Mod.Phys. E **23**, 1430008 (2014).
- [5] R. Poberezhnyuk, M. Gazdzicki, M.I. Gorenstein, Acta Physica Polon., B **46**, 1991 (2015).
- [6] K. Werner, F.-M. Liu, t. Pirog, Phys.rev. C **74**, 044902 (2006).
- [7] <https://web.i kp.kit.edu/rulrich/crmc/html>
- [8] S. Bass, et al., Prog.Part.Nucl.Phys. **41**, 255 (1998).

- [9] M. Blreicher, et al., J.Phys. G **25**, 1859 (1999).
- [10] Z.-W. Lin, et al., Phys.Rev. C **72**, 06490 (2005).
- [11] Z.-W. Lin, Phys.Rev. C **90**, 014904 (2014).
- [12] B. Zhang, et al., Phys.Rev. C **61**, 067901 (2000).
- [13] W. Cassing, E.L. Bratkovskaya, Phys.Rev. C **78**, 034919 (2008).
- [14] W. Cassing, E.L. Bratkovskaya, Nucl.Phys. A **831**, 215 (2009).
- [15] J. Mohs:, S. Ryu, H. Elfner, J.Phys. G **47**, 065101 (2020).
- [16] J. Weil, et al., Phys.Rev. C **94**, 054905 (2016).
- [17] A. Acharya, et al., (NA61/SHINE Collaboration) Eur. Phys. j. C **81**, 73 (2021).
- [18] Maja Mackowiak-Pawłowska for the NA61/SHINE Collaboration, arXiv:2112.01877 [nucl-ex].
- [19] A. Acharya *et al.*, (NA61/SHINE Collaboration), Eur. Phys. J. C **81**, 397 (2021)
- [20] A. Aduszkiewicz, et al., (NA49 Collaboration) Phys.Rev.C **102**, 011901(R) (2020).
- [21] G.I. Lykasov, A.I. Malakhov, A.A. Zaitsev, Eur. Phys. J. A **57** , 78 (2021).
- [22] A.M. Baldin, L.A. Didenko, Fortsch.Phys. **38**, 261 (1990).
- [23] A.M. Baldin, A.I. Malakhov, and A. N. Sissakian, Phys. Part. Nucl. **29** (Suppl. 1), 4 (2001).
- [24] A. M.Baldin, A. A. Baldin. Phys. Particles and Nuclei, **29** No3, 232 (1998).
- [25] A.M. Baldin, A.I. Malakhov. JINR Rapid Communications, No.1(87)-98, pp.5-12 (1998).
- [26] Baldin A.A. JINR Rapid Comm. No. 4[78]-96 p.61-68.
- [27] E. Fermi, Phys. Rev. **92**, 452 (1953)

- [28] I. Ya. Pomeranchuk, *Izv. Dokl. Akad. Nauk Ser.Fiz.* **78**, 889 (1951).
- [29] L.D. Landau, *Izv. Akad. Nauk Ser. Fiz.* **17**, 51 (1953).
- [30] R. Hagedorn, *Supplemento al Nuovo Cimento* **3**, 147 (1965).
- [31] D.A. Artemenkov, G.I. Lykasov, A.I. Malakhov, *Int.J.Mod.Phys.* **A30**, 1550127 (2015)
- [32] G.I. Lykasov, A.I. Malakhov, *Eur. Phys. J. A* **54**, 187 (2018).
- [33] A.I. Malakhov, G.I. Lykasov, *Eur. Phys. J. A* **56**, 114 (2020).
- [34] A.M. Abdulov, H. Jung, A.V. Lipatov, G.I. Lykasov, M.A. Malyshev, *Phys.Rev.* **D98**, 054010 (2018).
- [35] V.A. Bednyakov, A.A. Grinyuk, G.I. Lykasov, M. Pogosyan, *Int.J.Mod.Phys.*, **A27**, 1250042 (2012).
- [36] A.A. Grinyuk, G.I. Lykasov, A.V. Lipatov, N.P. Zotov, *Phys.Rev.* **D87**, 074017 (2013).
- [37] A.V. Lipatov, G.I. Lykasov, N.P. Zotov, *Phys.Rev.* **D89**, 014001 (2014).
- [38] A.M. Abdulov, H. Jung, A.V. Lipatov, G.I. Lykasov, M.A. Malyshev, *Phys.Rev.* **D98**, 054010 (2018).
- [39] N. Cartiglia, arXiv:1305.6131 [hep-ex].
- [40] S.H. Stark, *Eur.Phys.J. (Web of Conf.)* **141** 03007 (2017).
- [41] E. Schnedermann, J. Sollfrank, U. Heinz, *Phys.Rev.* **C48**, 2462 (1993).
- [42] G. Wilk, Z. Wlodarczyk, *Phys.Lett.* **84**, 2770 (2000).
- [43] K.A. Bugaev, *J.Phys.G:Nucl.Phys.*, **28**, 1981 (2002).
- [44] K.A. Bugaev, M. Gadzicki, M.I. Gorenstein, *Phys.Lett.* **B544**, 127 (2002).
- [45] J. Cleymans, G.I. Lykasov, A.S. Parvan, et al., *Phys.Lett. B* **723**, 351 (2013).
- [46] J.L. Kley, et al., E895 Collaboration, *Phys.Rev. C* **68**, 054905 (2003).

- [47] N. Abgrall, et al., NA61/SHINE Collaboration, Eur. Phys. J. C **74**, 2794 (2014).
- [48] K.A. Ter-Martirosyan, Sov.J.Nucl.Phys., **44**, (1986) 817.
- [49] A.Adiszkiewicz, *et al.*, (NA61/SHINE Collaboration) Phys.Rev.C **102** 1, 011901 (2020).
- [50] B. I. Abelev *et al.* (STAR Collaboration) Phys. Rev. C **79**, 034909 (2009).
- [51] A. Adare *et al.* (PHENIX Collaboration) Phys. Rev. C **83**, 064903 (2011).
- [52] Aamodt K. *et al.* (ALICE Collaboration) Eur. Phys. J. C **71**, 1655 (2011).
- [53] J. Adam *et al.* (ALICE Collaboration) Eur. Phys. J. C **75**, 226 (2015).
- [54] A. Acharya *et al.*,(NA61/SHINE Collaboration), Eur. Phys. J. C **80**, 961 (2020).